MECHANICAL PROPERTIES, MICROSTRUCTURE, AND TEXTURE OF ELECTRON BEAM BUTT WELDS IN HIGH PURITY NIOBIUM

H. Jiang[*], T.R. Bieler[*], C. Compton, T.L. Grimm

*Chemical Engineering and Materials Science, National Superconducting Cyclotron Laboratory
Michigan State University, East Lansing, MI 48824, USA

Abstract

The effects of Electron Beam Welding on solidification microstructure, texture, microhardness and mechanical properties were investigated in high purity Niobium weld specimens. The welds have an equiaxed microstructure with a 1 mm grain size in the fusion zone, 100 μm in the heat affected zone (HAZ) and 50 μm in the parent metal. The fusion zone had slightly higher microhardness values despite having a large grain size, while the unaffected material had the lowest microhardness. The texture in the weld consisted of a strong {111} fiber texture in the center and a mix of {111} - {100} components on the surface. Tensile tests of specimens gave σ_y = 60 MPa, but the UTS and elongation for weld specimens were lower than the parent material (137 vs. 165 MPa, 32% vs. 58%). The properties and microstructure of the weld are discussed in terms of optimizing the SRF cavity.

INTRODUCTION

Superconducting radio frequency (SRF) cavities made from high purity niobium are often fabricated using deep drawing metal forming processes to make parts that are subsequently welded together [1,2]. Electron beam welding (EBW) is used to obtain high quality welds that maintain the high purity required for superconductivity. Studies of EBW on pure metals have shown that properties of the weld material are comparable to the parent metal [3,4] although ductility was reduced and the grain size increased in Mg [3], and caused intergranular failure due to N segregation to boundaries in Mo [4]. However, little is known about how the electron beam weld affects the microstructure and properties that are important to high purity Nb SRF cavities.

Also, there is little published information on formability of pure niobium, but information on interstitial free (IF) or extra-low carbon steels [e.g. 5] may be transferable to pure niobium. Optimal processing for deep drawability in steels without developing undesirable surface roughness called "orange peel" involves rolling and recrystallization schedules that develop a very strong γ fiber texture, i.e. {111} ‖ sheet normal direction. This texture and a fine grain size minimizes the "orange peel" surface roughness which can be a source of flow instability that degrades formability [6]. Thus, this study is an initial investigation of interrelationships between welding and formability relevant to high purity niobium used for SRF cavities.

EXPERIMENTAL PROCEDURES

The niobium specimens used in this investigation were extracted by electro discharge machining (EDM) from 2 mm thick high purity niobium (RRR=150) sheet from Tokyo Denkai LTD. Two plates were butt welded together shown in Figure 1 using an electron beam weld procedure (1.7×10^{-5} torr, 50 kV, 46 mA, 5 mm/s, 1mm diameter, 1.5 mm circular oscillation). For one sheet, normal cleaning procedures were used [2] (ultra-sonically degreased ~20-30 min + cleaned in 60°C ultra-pure water ~45 minutes, dried in clean room, bagged with N_2; etched in BCP 5-7 min, rinsed in ultra-pure water just before welding), and in the less clean specimen, the final chemical etch was not done. Three 20 mm long samples were cut along the line indicated in Figure 1, and polished using standard techniques. Optical microscopy using a Nikon Epiphot 200 inverted microscope provided digital images from which the average grain size of the samples was determined using the linear intercept method and a known scale. Microhardness measurements were made using a LECO M-400-G1 hardness tester machine.
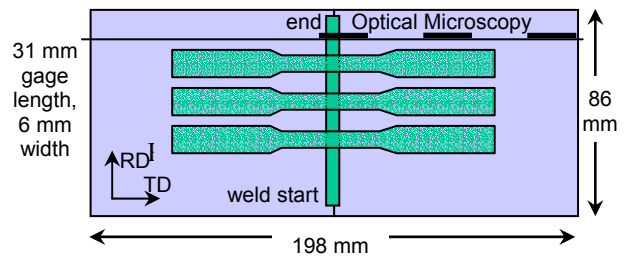

Figure 1: Welded plate and tensile specimens

Samples for texture measurements were prepared from as-received material to measure texture on the surface and near the midplane using a Scintag XDS 2000 diffractometer and popLA software for post processing the data [7]. The spatial distribution of texture through the thickness of weld samples was investigated with a *hkl Technologies* electron backscattered diffraction pattern mapping system in a Camscan 44FE microscope, using a 25-kV beam and a specimen current of about 2.3 nA. The data were further analyzed using TexSEM Laboratories Orientation Imaging Microscopy (OIM) Analysis software version 3.0. Maps of crystal orientations covered the full 2 mm thickness of the specimen at several locations in the heat affected zone and unaffected parent material. Due to the large grain size in the weld region, 25 mm long line scans were made along sections parallel to the weld direction near the surface and in the center of the sheet to measure a statistically significant number of grain orientations.

Tensile tests were conducted according to guidelines in ASTM E8 standard test methods. The weld material

tensile specimens were machined so the tensile axis was transverse to the weld direction, and the weld was parallel to the rolling direction (RD). The EB weld region is about 5.6 mm wide, ~20% of the specimen's 31 mm gage length. Specimens of the parent material were also deformed in the same conditions to compare with the weld specimens. The tensile tests were performed on a series 4200 Instron testing machine, model number 43K2. Deformation of weld specimens was periodically stopped to measure the actual thickness and width at several locations along the gage length.

RESULTS

Figure 2 shows the fusion zone of the weld. The lighting used illustrates solidification ridges and a large grain size in the weld. From optical micrographs, the grain size decreased with the increasing distance from the weld as shown in Figure 3.
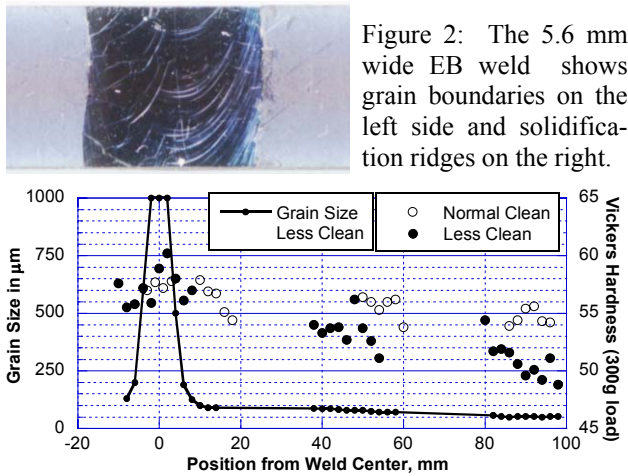

Figure 2: The 5.6 mm wide EB weld shows grain boundaries on the left side and solidifica-tion ridges on the right.

Figure 3: Grain size and Vickers Microhardness

Microhardness

The weld fusion zone has the highest microhardness value of ~57 H$_V$, and it decreased with increasing distance from the weld (Figure 3). The higher individual hardness values were correlated with indents on or near grain boundaries and the lower values were in the middle of a grain. Both samples show the same hardness in the weld fusion zone, but they have different rates of decreasing hardness with distance away from the weld.

Tensile Tests

The tensile properties of the as-received Niobium are comparable with prior work [2,8] and butt-weld specimens are illustrated with two specimens in Figure 4. The yield strength of as-received specimens was slightly higher than the butt-weld specimens, but the UTS of as-received specimens was ~30 MPa higher than butt-weld specimens, and the elongation was ~25% higher. The normal cleaning process caused a slight improvement in UTS and elongation of the weld specimens, but it may not be statistically significant.

The tensile tests were periodically stopped to measure the current width and thickness of the specimen in the

weld and HAZ regions. Deformation in these samples was predominantly in the width direction, and the thickness strain was nearly unchanged with strain after a small initial reduction, but it thinned during the final necking process prior to fracture. All of the weld specimens failed between the center and edge of the fusion zone, with orange-peel in the HAZ and very heterogeneous deformation shown in Figure 5. The analytically determined true stress-strain curve for the as-received parent material, and at three positions in the weld specimen (based upon the known loads and measured area changes) and the engineering stress-strain curves are plotted in Figure 4. The flow behavior in the weld fusion zone and the HAZ 10 mm from the center show the same yield stress values, but the fusion zone showed a lower strain hardening behavior, such that it became weaker
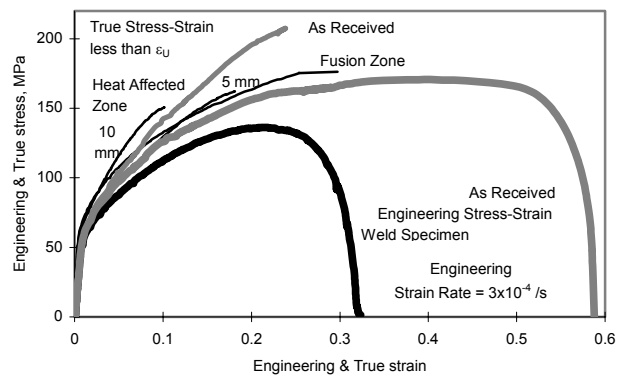
than the as-received material at a true strain of about 0.07.

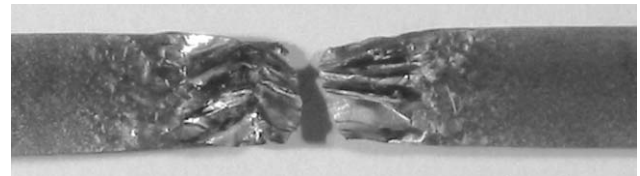Figure 4: Stress-Strain of weld and parent material

Figure 5: Fracture of weld specimen

Texture Analysis

The parent material texture in Figure 6 is shown as recalculated pole figures from the sample orientation distribution obtained using procedures given in [7]. The sheet center has a strong {111}<110> texture, but the near surface layer has a much weaker {111}<110> texture.
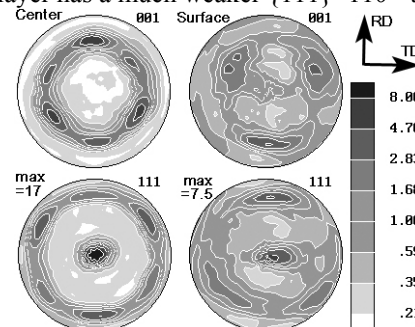

Figure 6: X-ray pole figure of parent material texture

Using OIM, microstructure and texture information were obtained simultaneously, as shown in the parent material scan in Figure 7. The orientations at the center show primarily <111> crystal directions aligned with the sheet normal direction, but the surface region has a variety of orientations, including <100> ∥ sheet normal. The pole figures obtained from OIM are consistent with the x-ray data, as shown in Table 1. Pole figures from the HAZ and the weld also show similar trends, indicating that solidification in the weld followed the texture in the parent material.
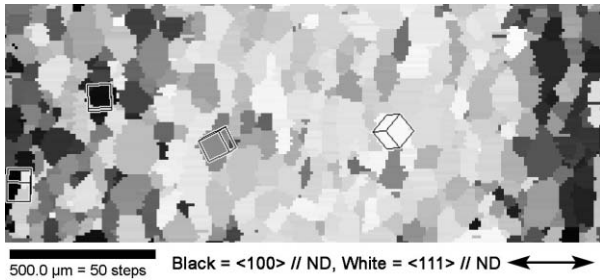

Figure 7: OIM scan of parent material; the full 2 mm sheet thickness is horizontal (sheet normal direction)

Table I: Maximum {111} Pole Figure Texture, x random, from OIM; surface / through thickness / center

Weld center	5mm HAZ	13 mm HAZ	Parent
10/-/14	13.9/13/18.2	6.2/8.3/14.1	5.4/8.0/12.2

DISCUSSION

The mechanical properties of the weld and HAZ are different from the parent material (Figure 4), due to differences in microstructure and impurity atom content. A slight increase in impurities in the weld is likely due to adsorbed water and oxygen on the surface. In the fusion zone, impurities would be well mixed since diffusion is rapid in the liquid phase. In the HAZ 5 mm from the center, where the grain size is large, there was probably about 10 seconds near the melting temperature, allowing for about 0.2 mm characteristic diffusion distance ($x = \sqrt{Dt}$; $D = 0.586\exp(-13188/T)$ mm^2/s, t=10s, 2741K [9]), so there was less mixing of oxygen in the HAZ than the fusion region, and even less diffusion into the material 10 mm from the center. Table II shows how the combination of impurity atom concentration and grain size based upon the Hall-Petch equation for the yield stress, $\sigma_y = \sigma_0 + kd^{-1/2}$ (k is a material constant and d is the grain size) may account for the observed flow in the weld specimen.

Texture measurements show that as-received niobium has very strong {111} texture in the center of samples, and some near-{100} texture near the surface of samples, similar to recrystallized IF steels [5]. The fact that the texture in the weld is similar to the texture in the parent material implies that resolidification occurred epitaxially with the existing grains in the solid adjacent to the melt pool. The large equiaxed grains in the weld and immediately adjacent HAZ imply that grain growth took place while the weld was cooling. The increasing intensity of the {111} texture as one gets closer to the weld is due to the increasing grain size.

The strong {111} texture is desirable for good formability because it provides a high "R" value for sheet metal forming and deep drawing [5]. This texture resists thinning, as indicated in the lack of thinning in the weld. This retention of the {111} texture in the weld is beneficial since even though a weld may be weaker than the parent material; its resistance to thinning will prevent unstable deformation in a welded structure.

The concerns important for applications to SRF cavities are the large grain size, the mixed surface texture components, and absorption of impurities. Impurities are known to disrupt the superconducting behavior, and the large grain size causes much greater orange peel effects if subsequent plastic deformation is required. The large grain size leads to surface roughness if any plastic deformation is imposed, due to the orange peel effect [6]. The different grain directions normal to the surface cause differential etching rates that lead to ledges at grain boundaries that can disrupt the superconducting state due to local aberrations in the magnetic field. Furthermore, the work function is a strong function of crystal orientation, so that electron emission will occur most on {100} oriented grains, and least on {110} grains [10]. Impurities can locally poison the superconducting state, leading to localized heating and electric field anomalies. All of these issues will assist quenching of the electric field due to emission or field disturbances. Thus, obtaining a material with surface texture that has no {100} fiber texture would be a desirable outcome for optimized high purity niobium for SRF cavities.

Table II: Impurity and Grain Size (GS) Effects

Location	Comments; n = dlnσ_T/dlnε_T (hardening rate), σ_y = yield stress, MPa, σ = flow stress
Parent	n=0.4, σ_y=60; Smallest GS => high n, lowest impurities => low σ
10 mm HAZ	n=0.4, σ_y=61; Smaller GS => high n like parent; some impurities => higher σ_y and σ
5 mm HAZ	n=0.4, σ_y=58; Larger GS => reduces σ_y, but higher impurities => higher σ_y
Fusion zone	n=0.3, σ_y=59; Largest GS => lowest n, σ, σ_y, but highest impurities => higher σ_y

REFERENCES

[1] F Smith, J Milewski, Welding Journal (USA) 80 (2001) 43.
[2] H Padamsee, J Knobloch, T Hays, in RF Superconductivity for Accelerators, Wiley & Sons, NY, (1998), p. 105.
[3] T Asahina, H Tokisue, Materials Transactions (Japan) 42 (2001) 2345.
[4] F Morito, Journal de Physique (France) 51 (1990) 281.
[5] N Hashimoto, N Yoshinaga, T Senuma, ISIJ International (Japan) 38 (1998) 617.
[6] R Orsund, O Lohne, Mater. Sci. Forum 94 (1992) 753.
[7] JS Kallend, UF Kocks, AD Rollett, H-R Wenk, Materials Science and Engineering A132 (1991) 1.
[8] MG Rao and P Knesisel, Mechanical Properties of high RRR Nb, DESY Print, TESLA 95-09, March 1995.
[9] Smithells Metals Reference Book, 7th ed., Butterworth Heinemann, Oxford, 1992, p. 13-90.
[10] CRC Handbook of Chemistry and Physics, 73rd ed., 1992, pp. 12-108f.